Supporting information

Photocatalysis, terahertz time domain spectroscopy and weak interactions of six polyoxometalate-based lanthanide phosphine oxide complexes

Guan-Yu Jin, [†a] Lan Zhang, [†a] Fu-Zhen Hu, [†a] Yan-Lei Lu, [a] Cong Hu, [a] Ying-Yu Li, [a] Hong-Liang Han, [a] Jian-Ming Liu, [b] Yu-Ping Yang, [c] Qiong-Hua Jin[*a] and Xing-Ru Li[*a]

a.Department of Chemistry, Capital Normal University, Beijing 100048, China. E-mail: jinqh@cnu.edu.cn, jinqh204@163.com.

b.School of Mathematical Sciences, Peking University, Beijing 100871, China.

c.School of Science, Minzu University of China, Beijing 100081, China.

†Guan-Yu Jin, Lan Zhang and Fu-Zhen Hu contributed equally to this work.

Electronic Supplementary Information (ESI) available: crystal structure information, IR spectra and thermogravimetric analysis. CCDC 2090276, 2090280, 2090281, 2090282, 2174527, 2174528 See DOI: 10.1039/x0xx00000x

Caption of Figure

Fig. S1 (a) formation of 1D structure of complex **2a** by intermolecular hydrogen bonds bridging; (b) 1D chain structure formed by weak Mo-O···π interaction bridging in the stacking structure of complex **2a**; (c) intermolecular C-H···π interaction in the stacking structure of complex **2a**; (d) a 3D structure formed by three weak interactions of intermolecular hydrogen bonds, Mo-O···π and intermolecular C-H···π bridging in the stacking structure of complex **2a**. (omits some atoms)
Fig. S2 (a) formation of 1D structure of complex **3a** by intermolecular hydrogen bonds bridging; (b) 1D chain structure formed by weak Mo-O···π interaction bridging in the stacking structure of complex **3a**; (c) intermolecular C-H···π interaction in the stacking structure of complex **3a**; (d) a 3D structure formed by three weak interactions of intermolecular hydrogen bonds, Mo-O···π and intermolecular C-H···π bridging in the stacking structure of complex **3a**. (omits some atoms)
Fig. S3 (a) formation of 1D structure of complex **4a** by intermolecular hydrogen bonds bridging; (b) 1D chain structure formed by weak Mo-O···π interaction bridging in the stacking structure of complex **4a**; (c) intermolecular C-H···π interaction in the stacking structure of complex **4a**; (d) a 3D structure formed by three weak interactions of intermolecular hydrogen bonds, Mo-O···π and intermolecular C-H···π bridging in the stacking structure of complex **4a**. (omits some atoms)
Fig. S4 The IR spectra for complex **1a**.
Fig. S5 The IR spectra for complex **2a**.
Fig. S6 The IR spectra for complex **3a**.
Fig. S7 The IR spectra for complex **4a**.
Fig. S8 The IR spectra for complex **1b**.
Fig. S9 The IR spectra for complex **2b**.
Fig. S10 The IR spectra for complex **3b**.

Caption of Table

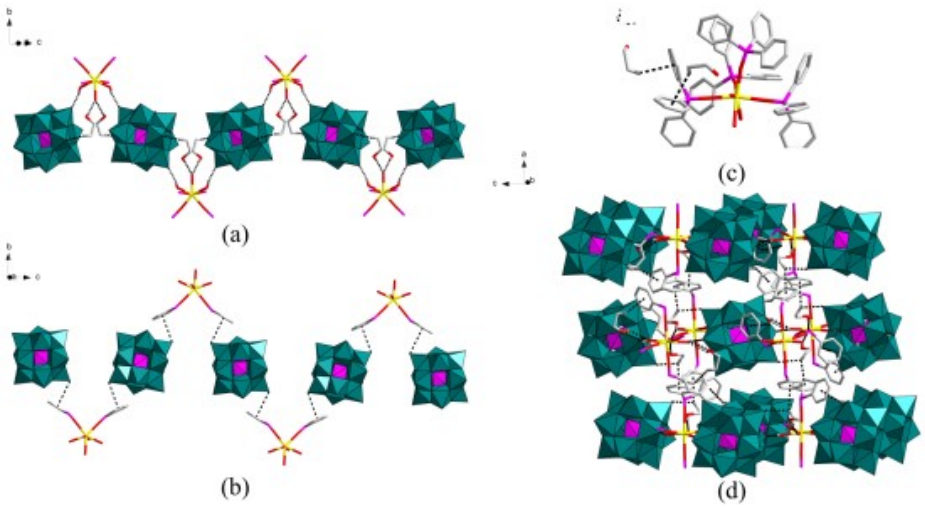

Fig. S1 (a) formation of 1D structure of complex **2a** by intermolecular hydrogen bonds bridging; (b) 1D chain structure formed by weak Mo-O···π interaction bridging in the stacking structure of complex **2a**; (c) intermolecular C-H···π interaction in the stacking structure of complex **2a**; (d) a 3D structure formed by three weak interactions of intermolecular hydrogen bonds, Mo-O···π and intermolecular C-H···π bridging in the stacking structure of complex **2a**. (omits some atoms)

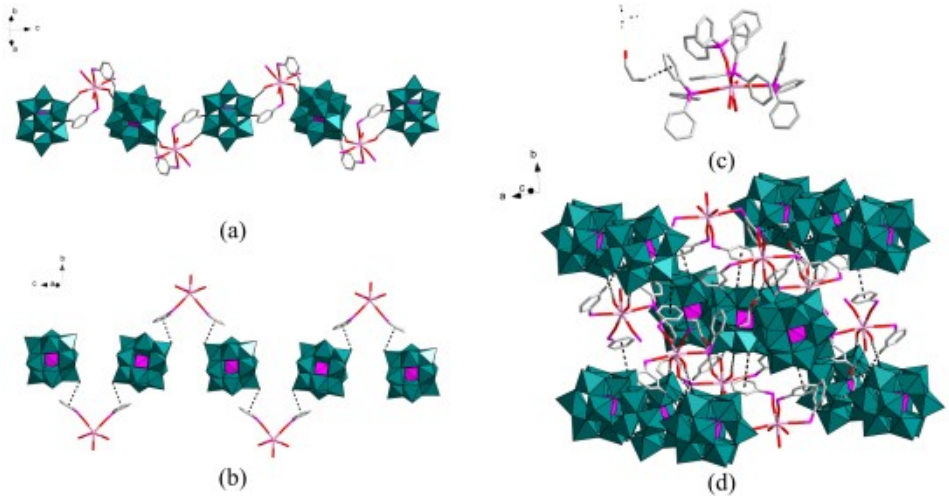

Fig. S2 (a) formation of 1D structure of complex **3a** by intermolecular hydrogen bonds bridging; (b) 1D chain structure formed by weak Mo-O···π interaction bridging in the stacking structure of complex **3a**; (c) intermolecular C-H···π interaction in the stacking structure of complex **3a**; (d) a 3D structure formed by three weak interactions of intermolecular hydrogen bonds, Mo-O···π and intermolecular C-H···π bridging in the stacking structure of complex **3a**. (omits some atoms)

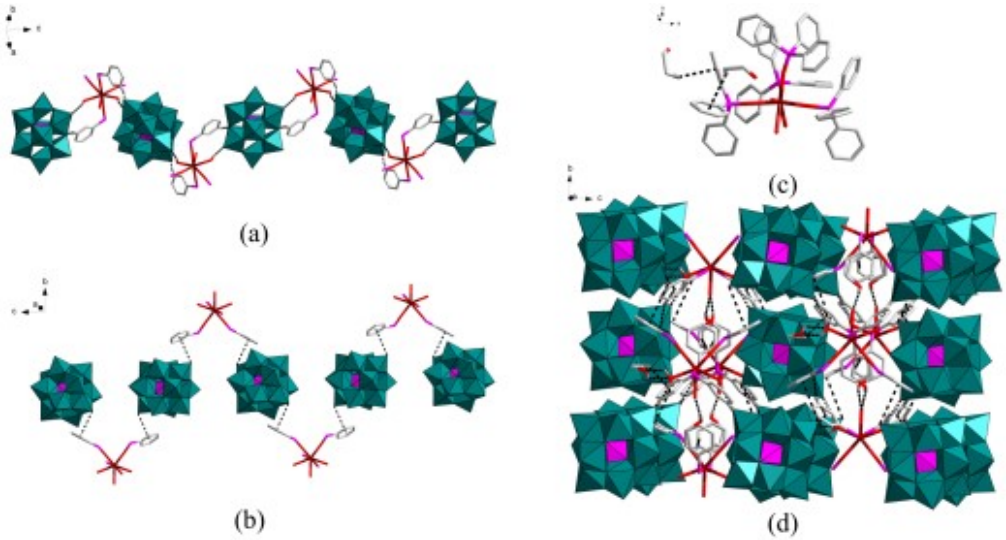

Fig. S3 (a) formation of 1D structure of complex **4a** by intermolecular hydrogen bonds bridging; (b) 1D chain structure formed by weak Mo-O···π interaction bridging in the stacking structure of complex **4a**; (c) intermolecular C-H···π interaction in the stacking structure of complex **4a**; (d) a 3D structure formed by three weak interactions of intermolecular hydrogen bonds, Mo-O···π and intermolecular C-H···π bridging in the stacking structure of complex **4a**. (omits some atoms)

IR spectra and thermogravimetric analysis

IR spectra of Keggin type polyoxometalates $H_3PMo_{12}O_{40}$ and complexes **1a-4a**, **1b** and **4b** were obtained by KBr pressing at room temperature (Fig. S4-S12). The infrared spectrum of $H_3PMo_{12}O_{40}$ shows the characteristic peak of Keggin structure in the range of 1100-600 cm^{-1}: P-O_a (1065 cm^{-1}), Mo =O_t (964 cm^{-1}), MO-O_b-Mo (890-850 cm^{-1}), MO-O_c-Mo (800-760 cm-1). For $OPPh_3$, the characteristic absorption peak of P=O bond stretching vibration is 1187 cm^{-1}, and the characteristic absorption peak generated by benzene ring vibration is 1641-1439 cm^{-1}, which is similar to the reported value.[48] For L ligands, the characteristic absorption peak of C-P-O bond stretching vibration is 1035 cm^{-1} and the characteristic absorption peak of P=O bond stretching vibration is 1260 cm^{-1}. Infrared spectra of **1a-4a, 1b** and **4b** showed that the characteristic vibration absorption peaks generated by $[PMo_{12}O_{40}]^{3-}$ and $OPPh_3$ and L ligands in these complexes were classified as vas (P-O_a), vas (Mo=O_t), vas (Mo-O_b-Mo) and vas (Mo-O_c-Mo). The four characteristic peaks appeared at: **1a**: 1065, 959, 881, 809 cm^{-1}; **2a**: 1065, 963, 882, 808 cm^{-1}; **2b**: 1065, 963, 881, 809 cm^{-1}; **4a**: 1065, 962, 881, 810 cm^{-1}; **1b**: 1063, 958, 880, 805 cm^{-1}; **2b**: 1063, 958, 879, 803 cm^{-1}; **3b**: 1063, 958, 880, 803 cm^{-1}; **4b**: 1063, 958, 880, 803 cm^{-1}. Compared with the IR spectra of $H_3PMo_{12}O_{40}$, the vas (Mo-Ob-Mo) and vas (Mo-Oc-Mo) characteristic peaks of **1a-4a** respectively moved to the high frequency region by about 12 cm^{-1} and 20 cm^{-1}, resulting in a blue shift, **1b**, **4b** respectively moved to the high frequency region by about 10 cm^{-1} and 14 cm^{-1}, resulting in a blue shift, which may be attributed to stronger interaction between metal ions.[49] The characteristic absorption peak of v (P=O) in complexes **1a-4a** is about 1124 cm^{-1}, and in complexes **1b** and **4b** are 1225, 1211, 1209, 1208 cm^{-1}. Compared with vas (P=O) in L, complexes **1b** and **4b** move about 63 cm^{-1} and 50 cm^{-1} to the low-frequency region and has a red shift, which confirme the coordination reaction between ligands and lanthanide ions. However, the different binding energies of ligands L and $OPPh_3$ with metal lead to different degrees of red shift or blue shift. $OPPh_3$ binds more stably to metal, which will be confirmed in the subsequent comparison.

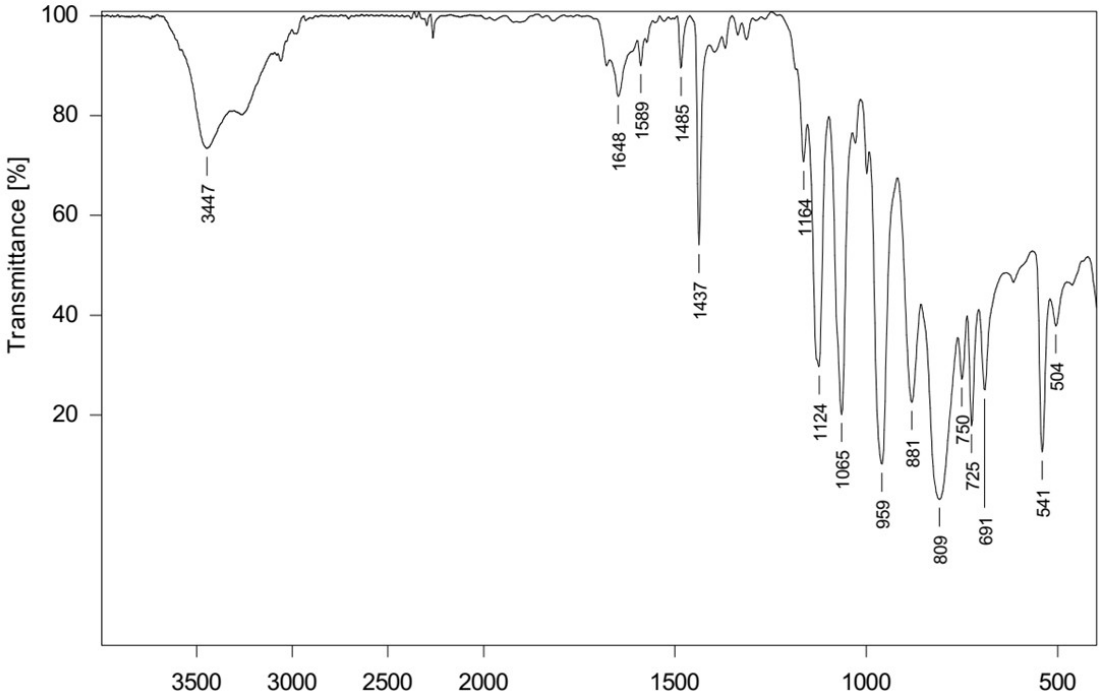

Fig. S4 The IR spectra for complex **1a**.

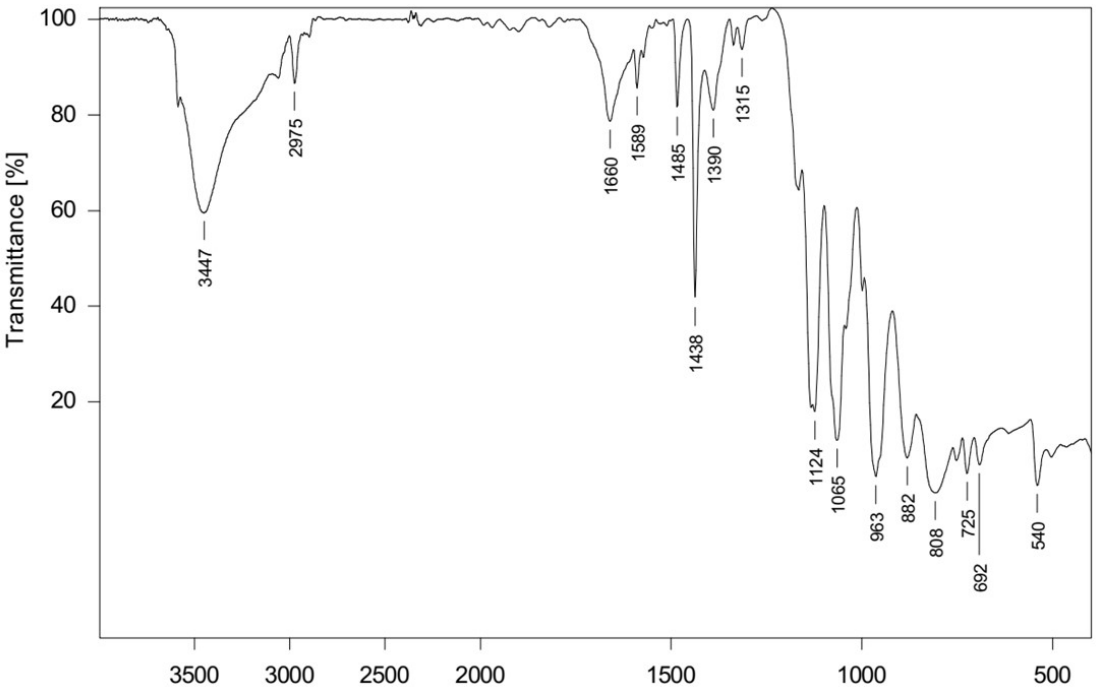

Fig. S5 The IR spectra for complex **2a**.

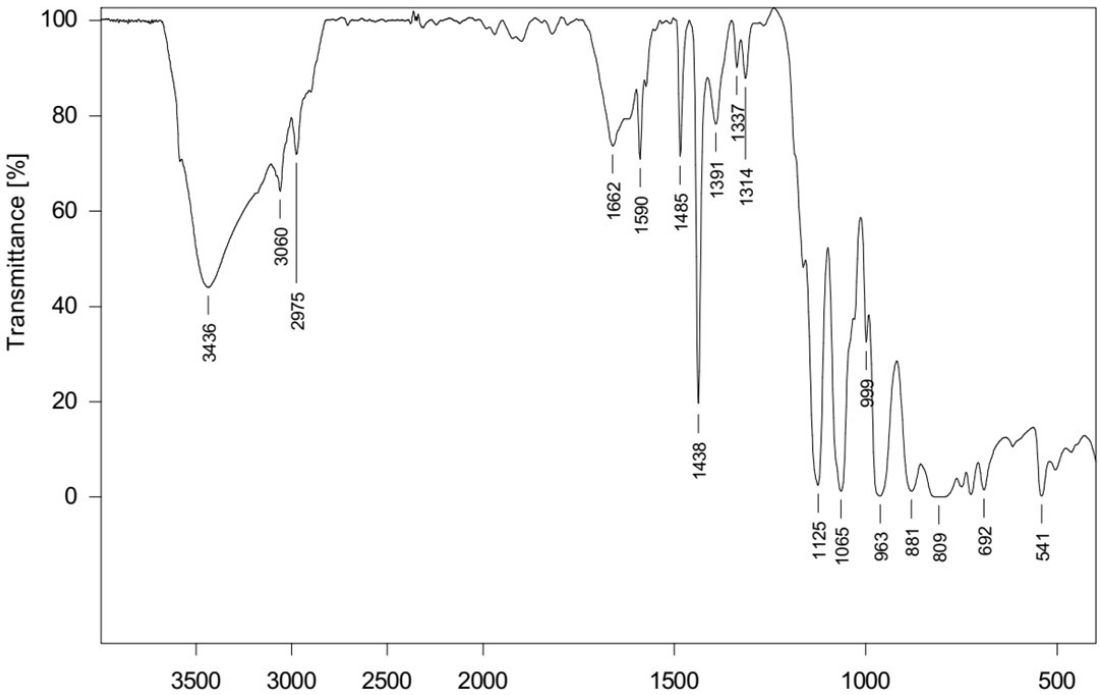

Fig. S6 The IR spectra for complex **3a**.

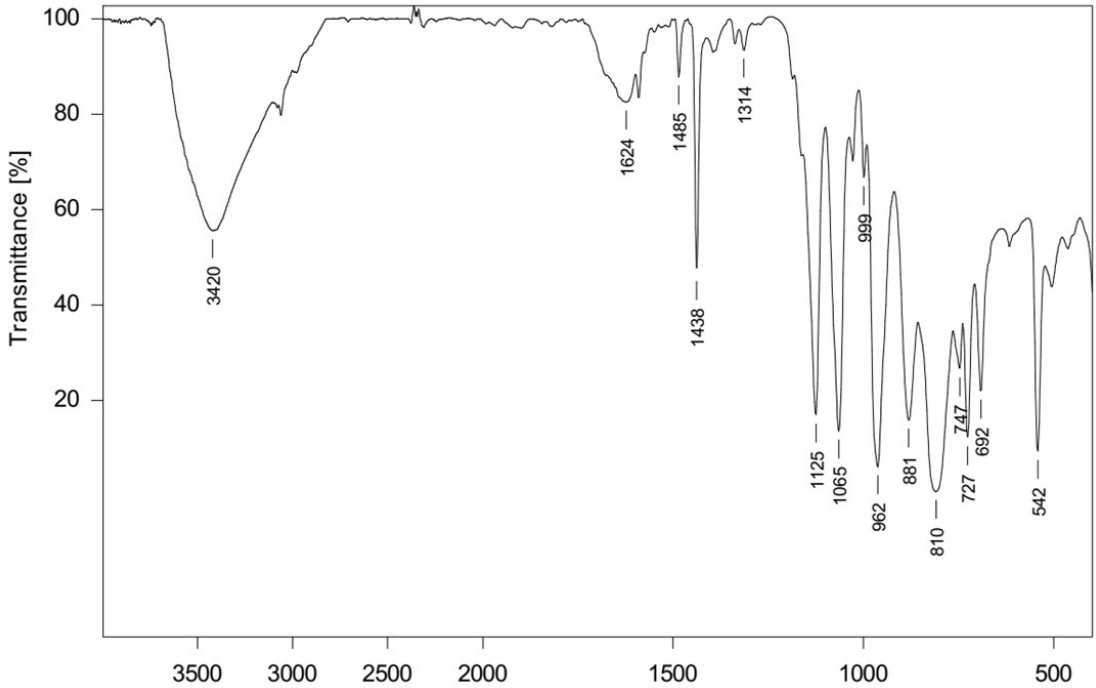

Fig. S7 The IR spectra for complex **4a**.

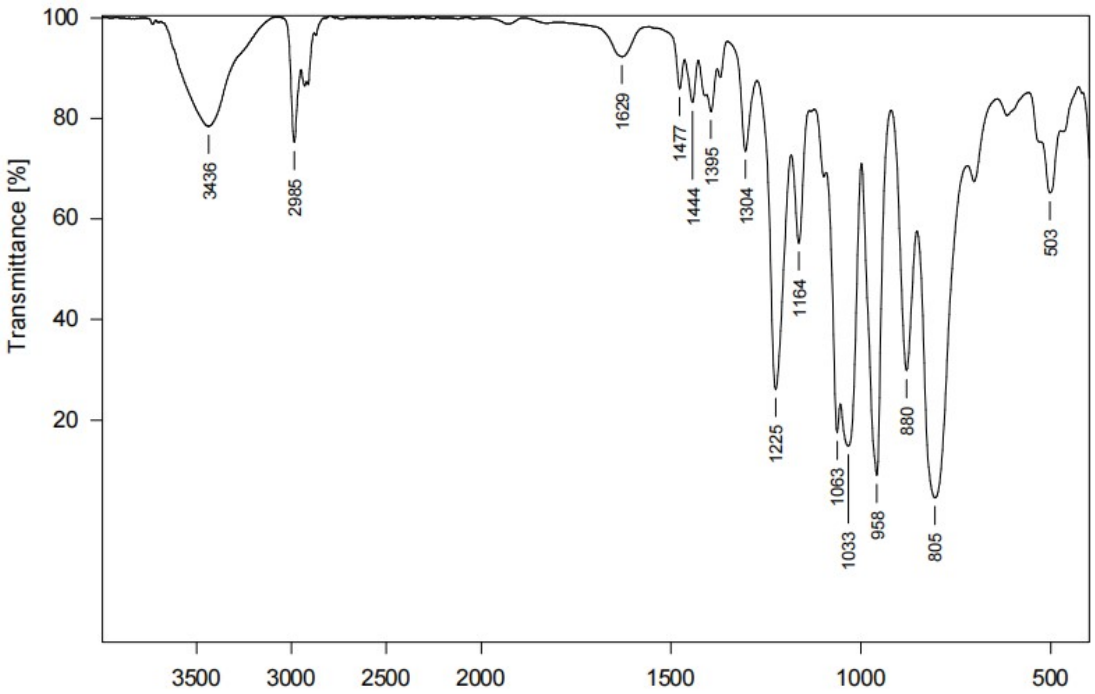

Fig. S8 The IR spectra for complex **1b**.

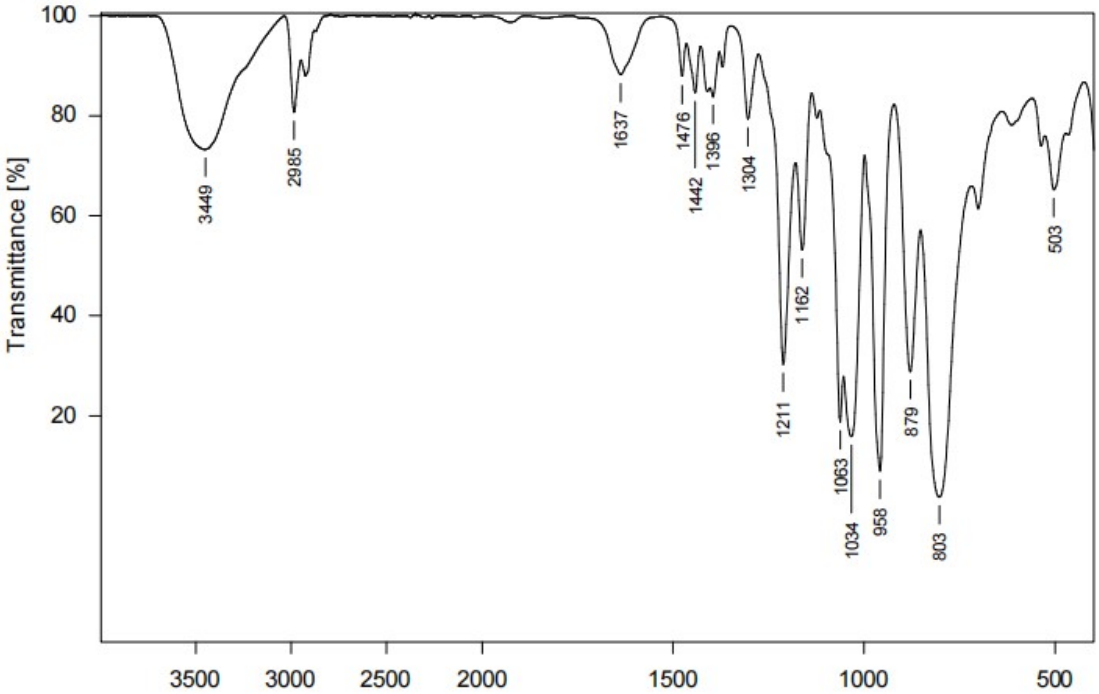

Fig. S9 The IR spectra for complex **2b**.

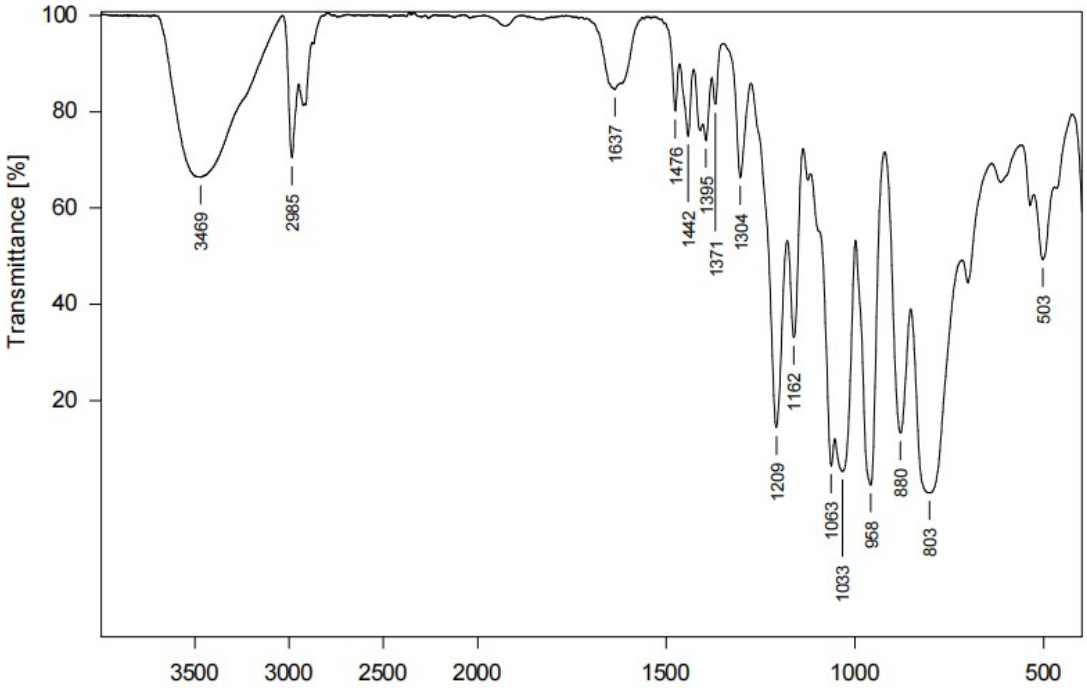

Fig. S10 The IR spectra for complex **3b**.

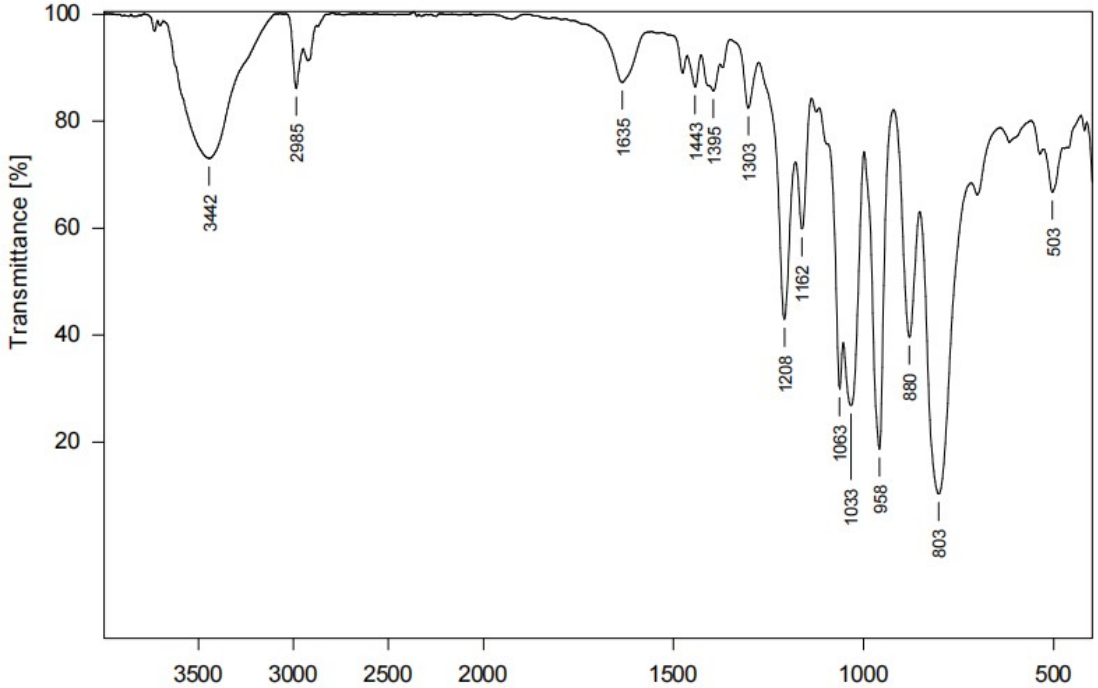

Fig. S11 The IR spectra for complex **4b**.

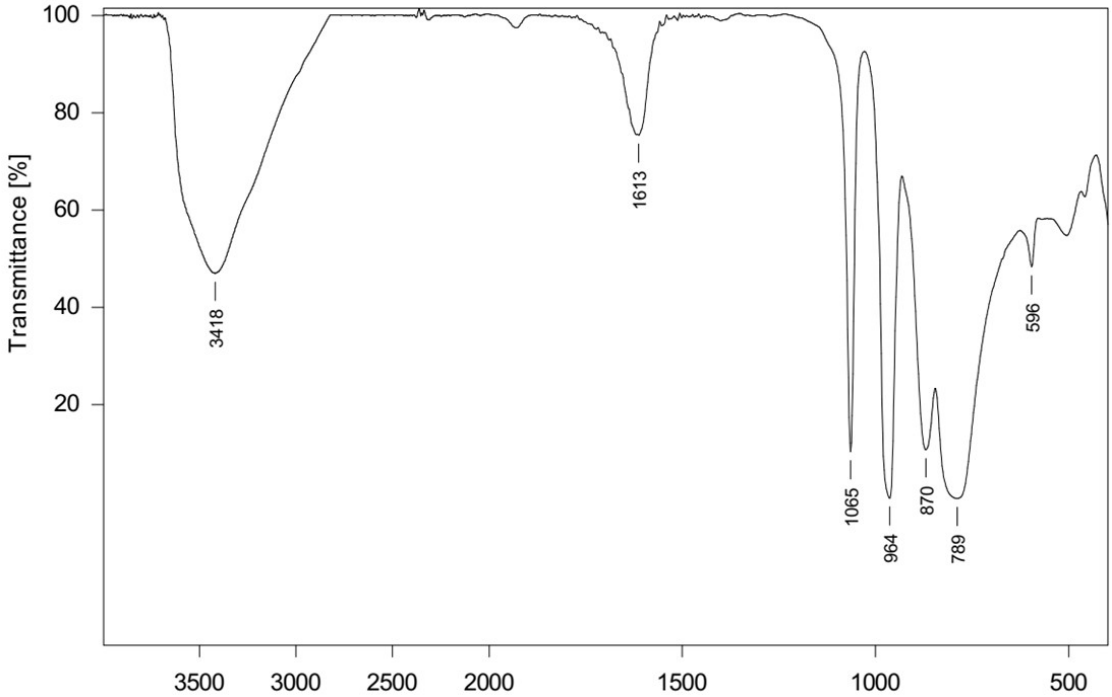

Fig. S12 The IR spectra for $H_3PMo_{12}O_{40}$.

The stabilities of complexes **1a**-**4a**, **1b** and **4b** were studied by thermogravimetric analysis (TGA). Since only lanthanide central ions and solvent molecules are different in complexes **1a**-**4a**, they have very similar thermogravimetric curves, as shown in Fig. S13. The initial slow weightlessness of complexes **1a**-**4a** in the range of 30-250 °C with 7.0% (calculated value: 6.6%), 6.8% (calculated value: 7.1%), 6.8% (calculated value: 7.1%), 6.2% (calculated value: 7.1%), respectively, which can be attributed to the loss of four acetonitrile or ethanol solvent molecules and three coordination water molecules in the lattice. Then a rapid and significant weight loss at 360-460 **°C**, with a weight loss of approximately 17.9%, mainly due to $[PMo_{12}O_{40}]^{3-}$ starting to decompose. $OPPh_3$ ligand begins to decompose at about 460 **°C**. The $[PMo_{12}O_{40}]^{3-}$ that has not been decomposed before continues to decompose, resulting in rapid and obvious weight loss of complexes **1a**-**4a** in the range of 460-800 **°C**. Complex **1b** has only a small weight loss in the range of 30-250°C because there is no crystalline coordination water in complex **1b** and only one solvent molecule. The initial slow weightlessness of complex **4b** in the range of 30-250 **°C** with 1.8% (calculated values: 2.0%), which can be attributed to the loss of one acetonitrile solvent molecule and one coordination water molecule in the lattice. A rapid and significant weight loss occurred at 250-290 **°C** with 14.77% and 10.19%, respectively, which was mainly due to $[PMo_{12}O_{40}]^{3-}$ starting to decompose. L ligand begins to decompose at about 290 **°C**, and the $[PMo_{12}O_{40}]^{3-}$ that has not been decomposed before continues to decompose, resulting in rapid and obvious weight loss of complexes **1b** and **4b** in the range of 290-800 **°C**.

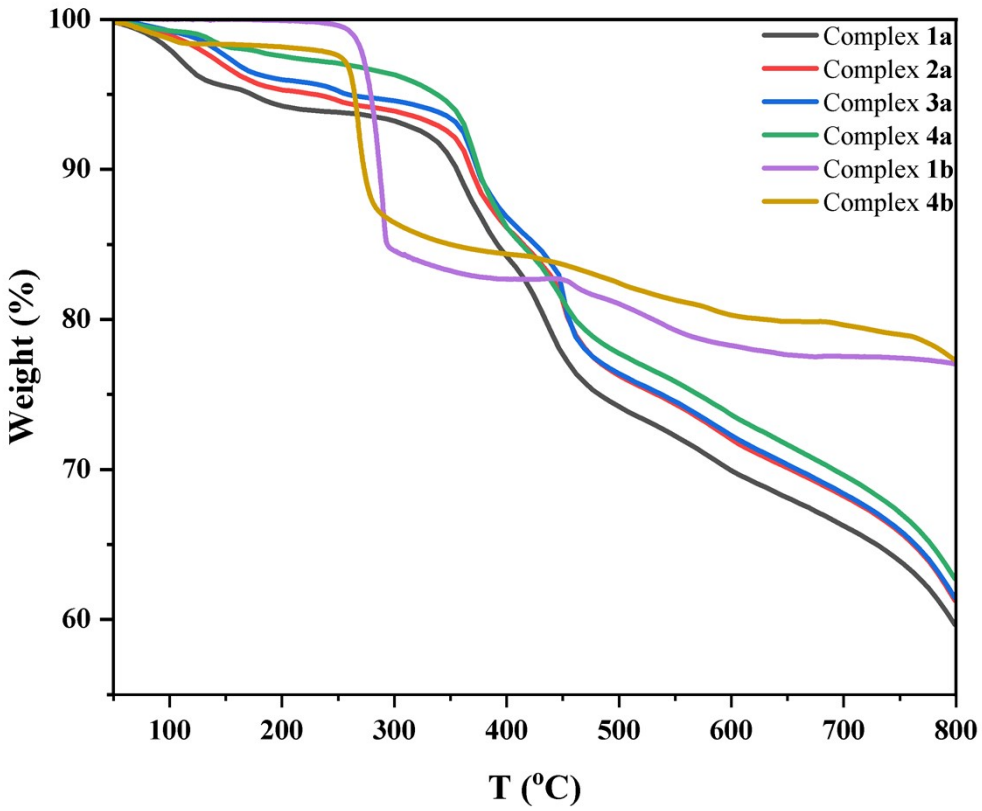

Fig. S13 Thermogravimetric curves of complexes **1a-4a**, **1b** and **4b**.

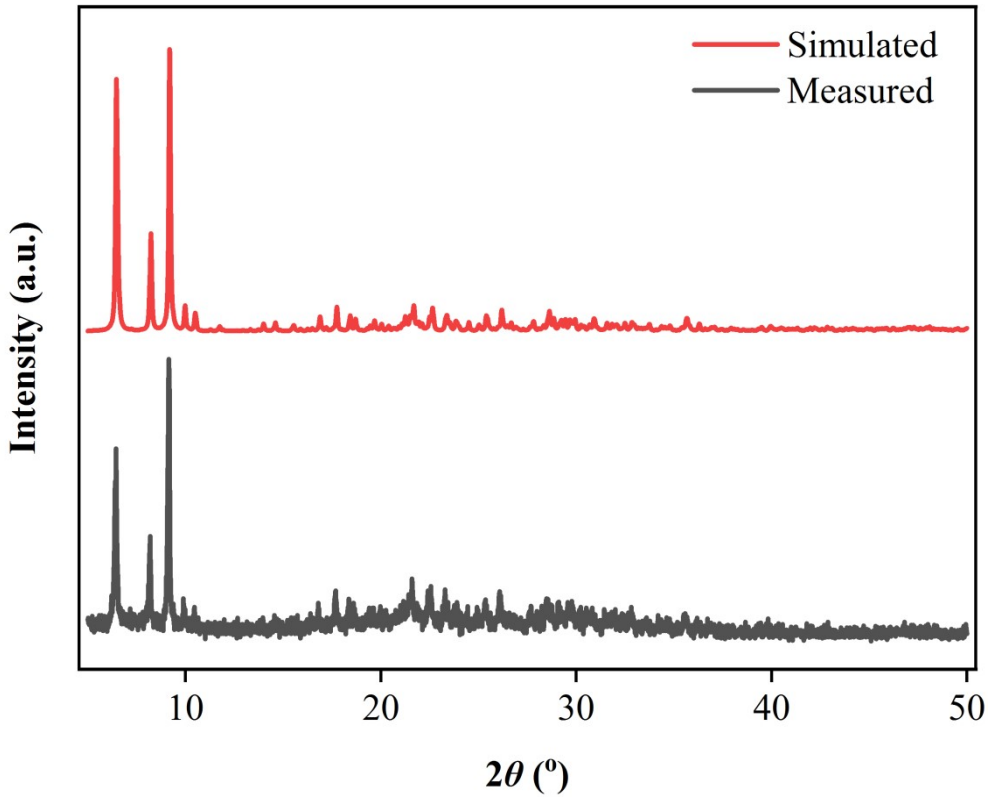

Fig. S14 Powder X-ray diffraction of complex **1a**

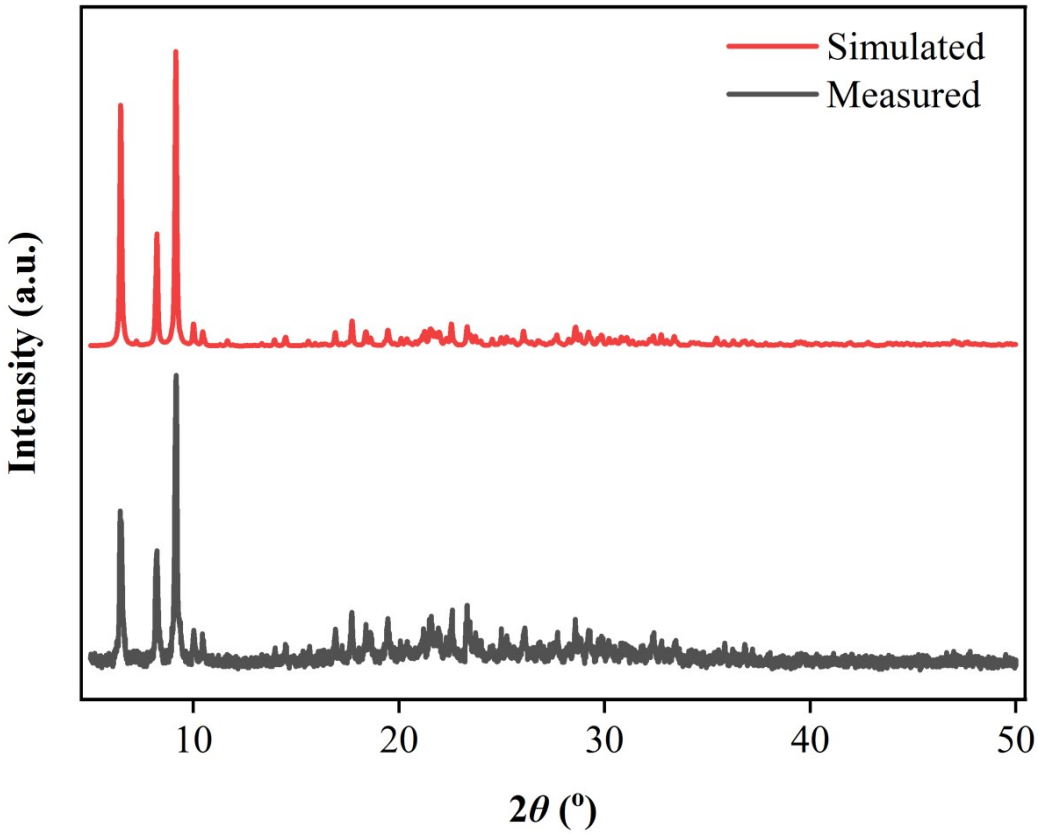

Fig. S15 Powder X-ray diffraction of complex **2a**

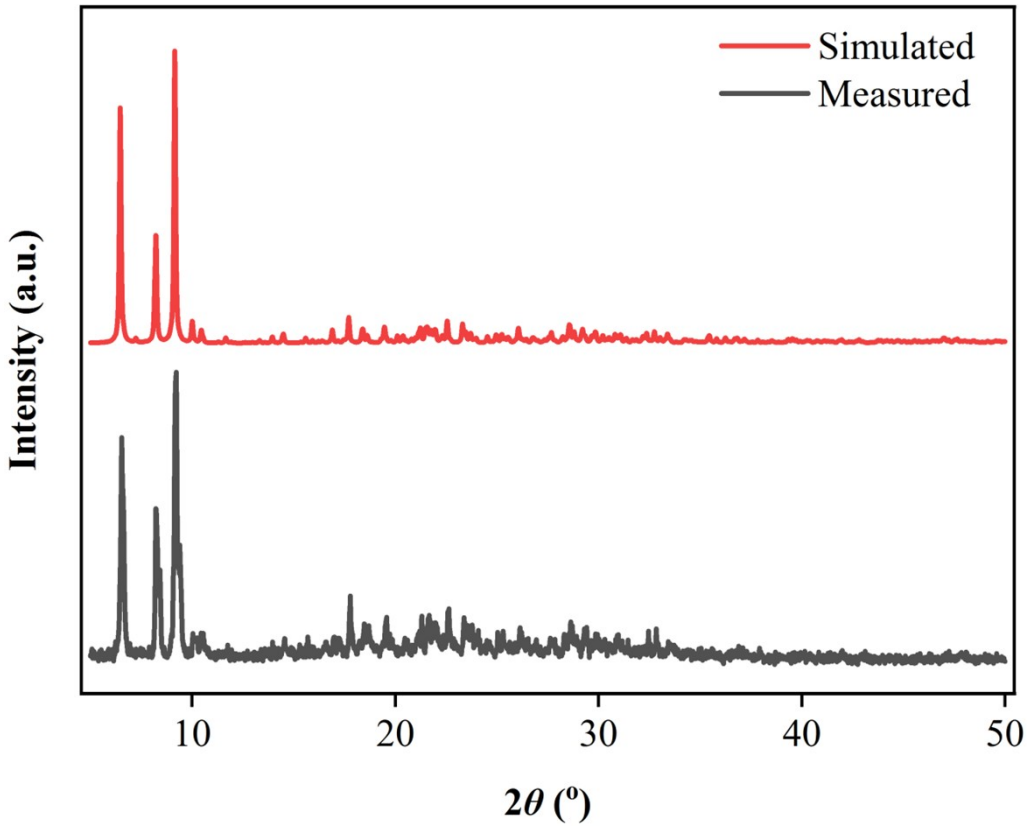

Fig. S16 Powder X-ray diffraction of complex **3a**

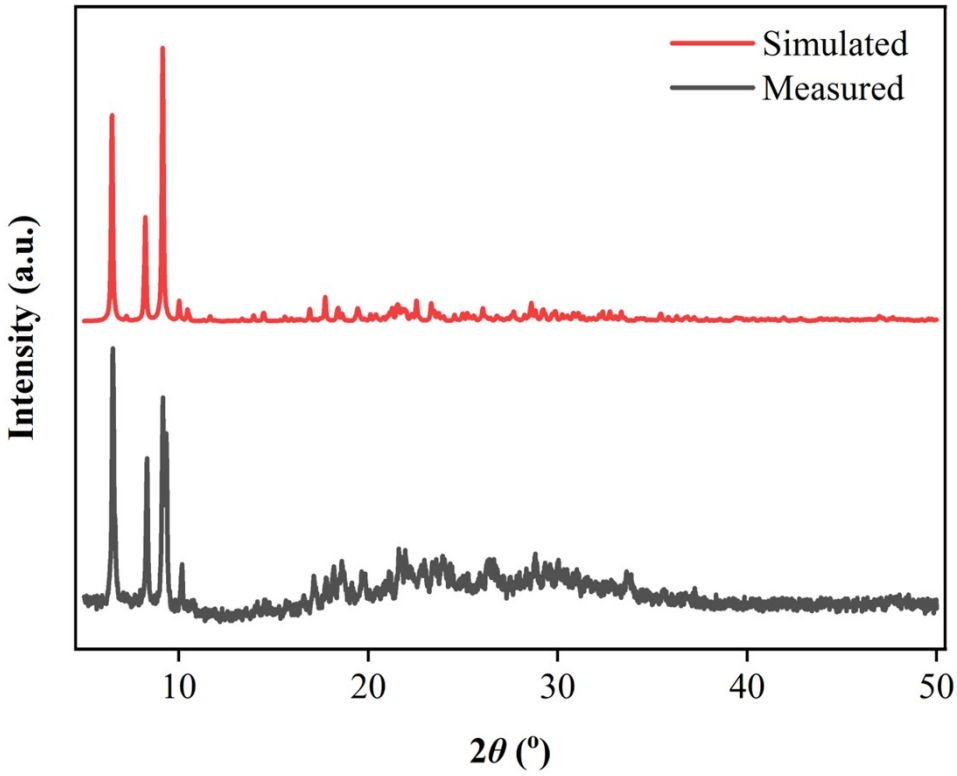

Fig. S17 Powder X-ray diffraction of complex **4a**

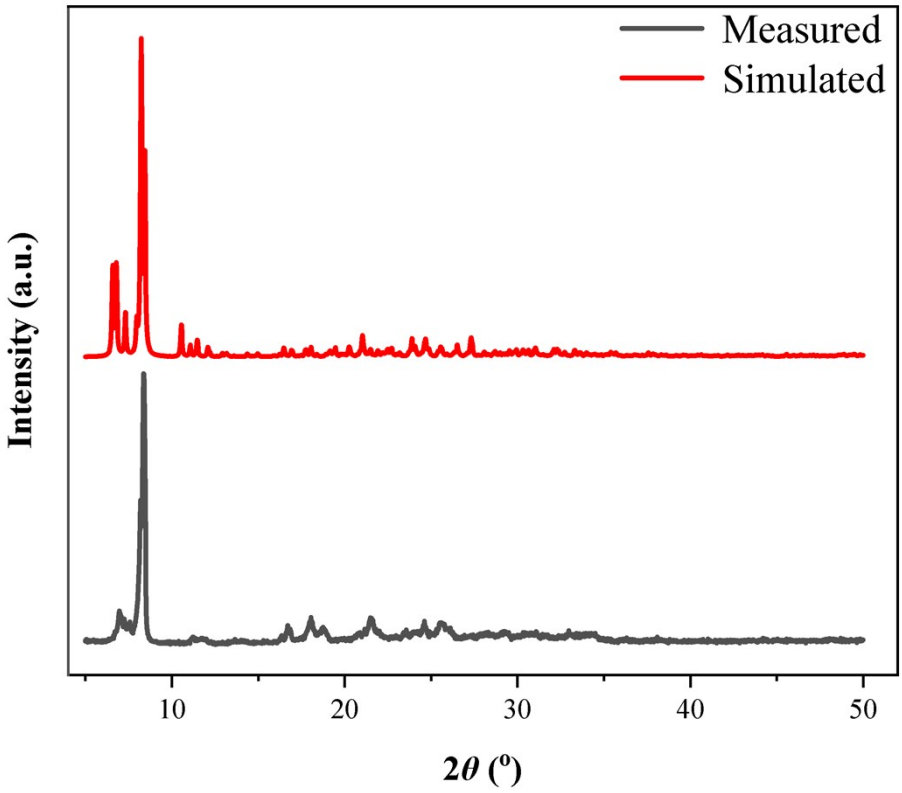

Fig. S18 Powder X-ray diffraction of complex **1b**

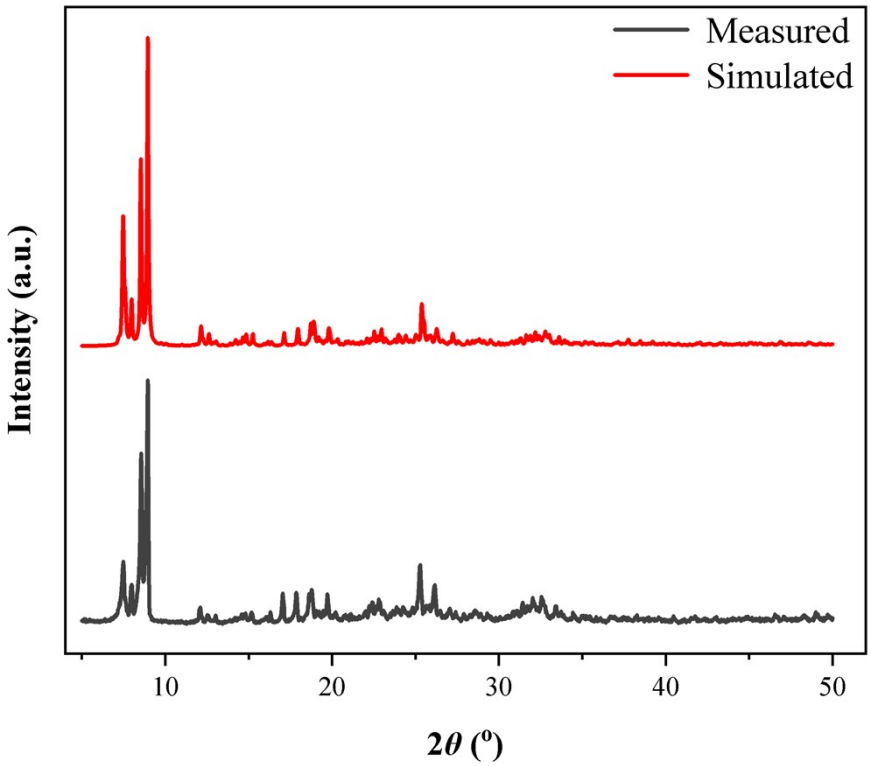

Fig. S19 Powder X-ray diffraction of complex **4b**

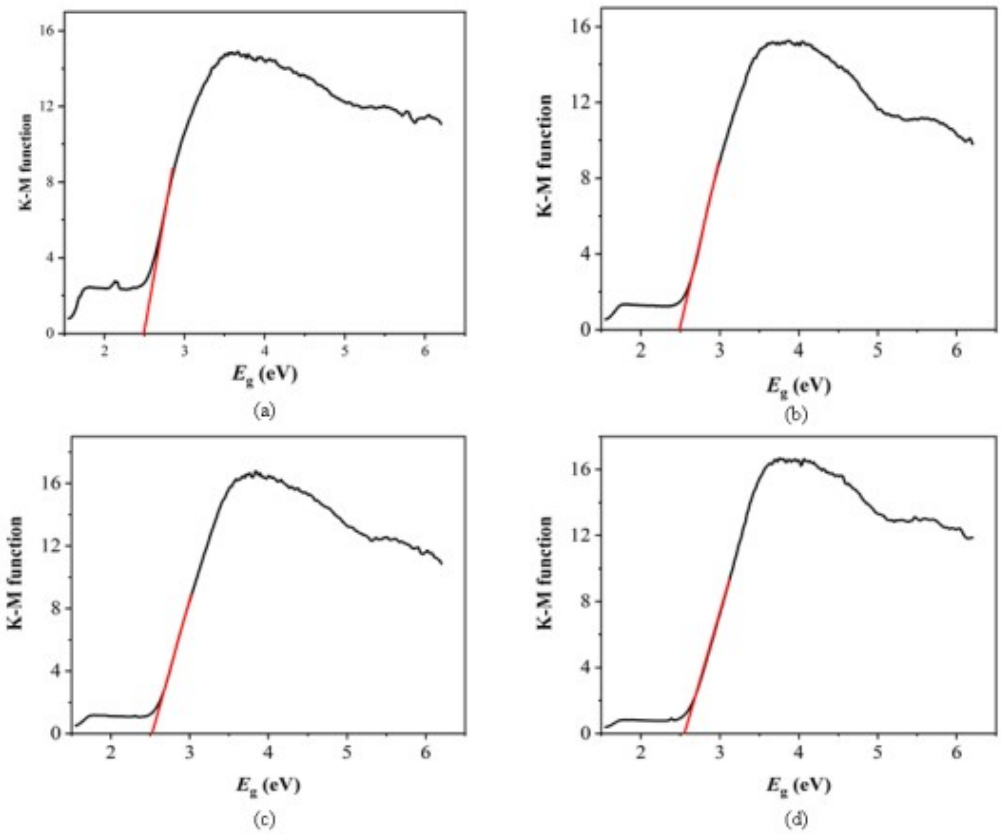

Fig. S20 Diffuse reflectance spectra of K-M function vs. *E* of complexes **1a-4a**.

Adsorption of dyes by complexes

Adsorption is a simple and effective method during the purification process of dye wastewater. Based on electrostatic interaction, RhB, as a cationic dye, can be effectively handled by large volume of $[PMo_{12}O_{40}]^{3-}$ added to the complexes. During the adsorption experiment, 1.5 mL of sample solution was collected at certain intervals, and UV-vis spectroscopy was performed after centrifugation at 10000 r/min. The results show that complexes **1b**, **4b** have excellent dye adsorption performance and RhB was adsorbed significantly within 5 minutes (Fig. S21-22). It is worth noting that among the two complexes, **1b** has the highest adsorption efficiency with the rate being 93.15% at 5 minutes, and reaching 94.51% after 30 minutes. In order to confirm that only adsorption but no degradation occurs, the samples after adsorption were soaked in ethanol, and the existence of RhB was proved by UV-vis spectroscopy. We also monitored the PXRD patterns after adsorption and desorption, indicating that the framework of **1b**, **4b** is stable and maintains during the processes.

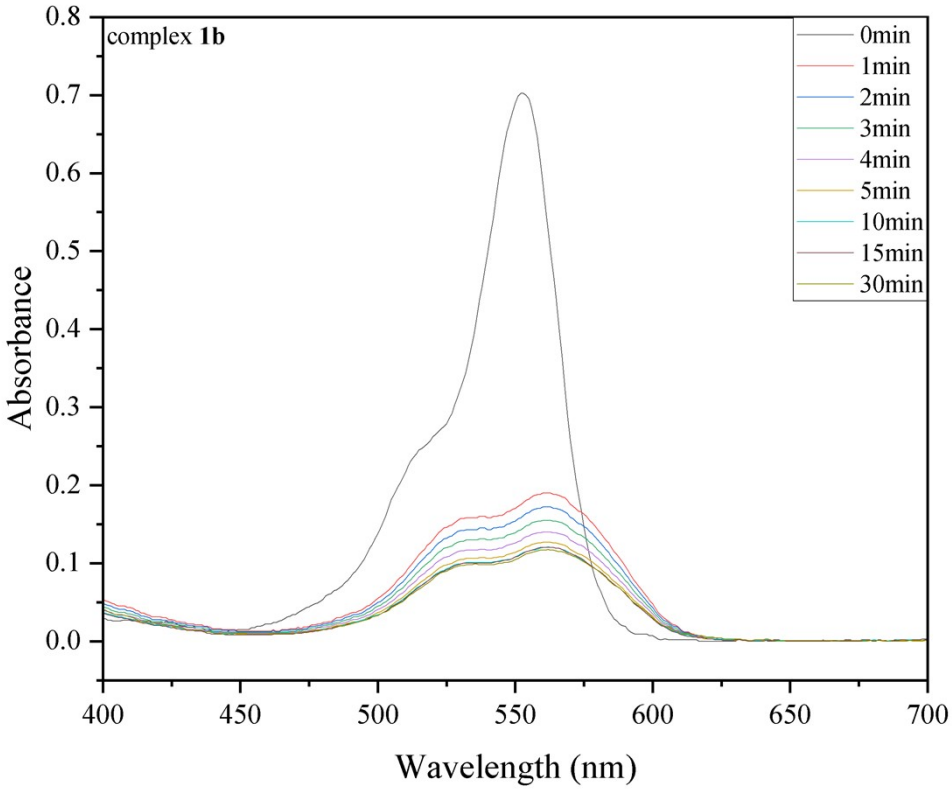

Fig. S21 UV-Vis spectra of RhB solutions under different adsorption time—**1b**

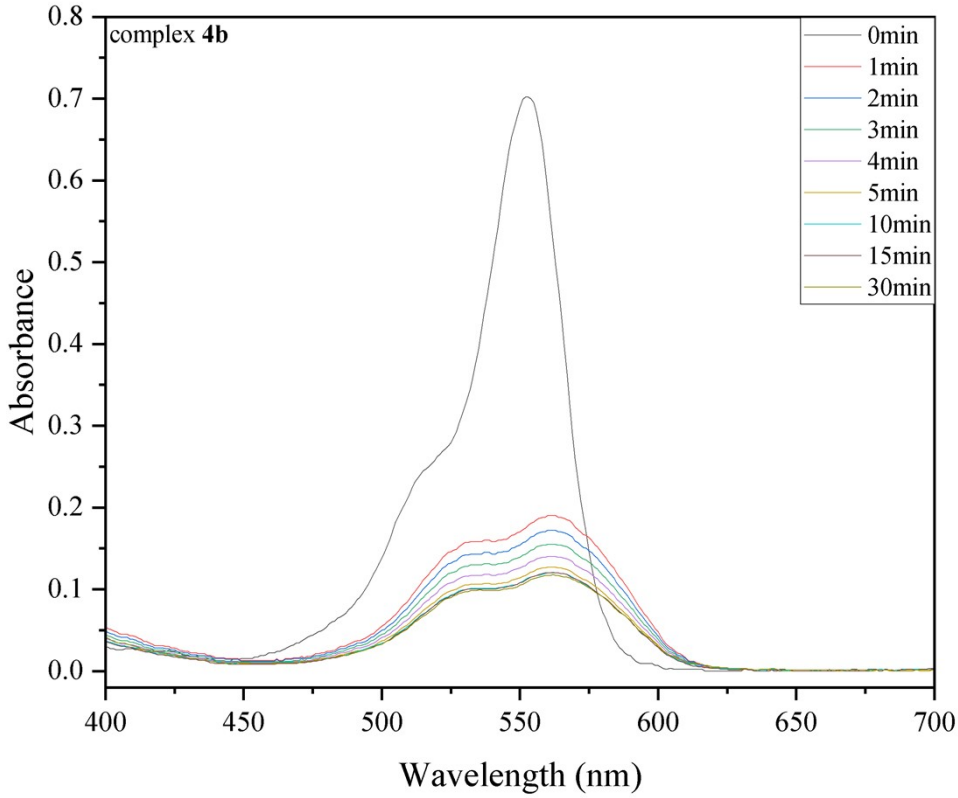

Fig. S22 UV-Vis spectra of RhB solutions under different adsorption time—**4b**

The two complexes have similar structures but different intermolecular interactions, leading to a small gap in their adsorption performance. It is speculated that the slight difference can be attributed to the difference in hydrogen bonds between molecules, especially the hydrogen bonds on the surface of $[PMo_{12}O_{40}]^{3-}$, which may affect the diffusion of dye molecules.

The characteristic peaks of these complexes are as follows:

$H_3PMo_{12}O_{40}$ (0.40, 0.53, 0.67, 0.73, 1.84, 1.98, 2.09, 2.19 THz);

$OPPh_3$ ligand (0.30, 0.41, 0.53, 0.80, 1.19, 1.58, 1.71, 2.04, 2.14, 2.27 THz);

L ligand (0.33, 0.36, 0.47, 0.56, 0.63, 0.73, 0.83, 1.03, 1.09, 1.19, 1.49, 1.66, 1.96, 2.02, 2.13, 2.29 THz);

Complex **1a** (0.38, 0.50, 0.63, 0.90, 1.04, 1.17, 1.31, 1.44, 1.57, 1.72, 1.84, 1.97, 2.10, 2.27 THz);

Complex **2a** (0.30, 0.40, 0.53, 0.67, 0.81, 0.93, 1.06, 1.19, 1.34, 1.61, 1.73, 1.84, 2.00, 2.26 THz);

Complex **3a** (0.29, 0.41, 0.52, 0.66, 0.81, 0.93, 1.04, 1.18, 1.30, 1.43, 1.71, 1.83, 1.97, 2.25 THz);

Complex **4a** (0.30, 0.41, 0.53, 0.67, 0.94, 1.05, 1.18, 1.31, 1.48, 1.60, 1.70, 1.82, 1.98, 2.16, 2.26 THz);

Complex **1b** (0.43, 0.69, 0.86, 0.96, 1.03, 1.22, 1.29, 1.36, 1.66, 1.79, 1.92, 2.13, 2.19, 2.26 THz);

Complex **4b** (0.35, 0.64, 0.90, 1.05, 1.34, 1.59, 1.74, 1.94, 2.13, 2.29 THz).

Table S1 Selected bond lengths (Å)and bond angles (°) for complexes **1a-4a, 1b** and **4b**.

1a					
Nd(1)-O(1)	2.345(8)	Nd(1)-O(2)	2.351(8)	Nd(1)-O(3)	2.486(8)
Nd(1)-O(4)	2.493(13)				
O(1)-Nd(1)-O(1)	167.4(4)	O(1)-Nd(1)-O(2)	90.2(3)	O(1)-Nd(1)-O(2)	99.1(3)
O(1)-Nd(1)-O(3)	81.8(3)	O(1)-Nd(1)-O(3)	93.4(3)	O(1)-Nd(1)-O(4)	83.7(19)
O(2)-Nd(1)-O(2)	85.0(4)	O(2)-Nd(1)-O(3)	152.7(3)	O(2)-Nd(1)-O(3)	70.7(3)
O(2)-Nd(1)-O(4)	137.5(19)	O(3)-Nd(1)-O(3)	135.4(4)	O(3)-Nd(1)-O(4)	67.7(2)
2a					
Dy(1)-O(23)	2.252(5)	Dy(1)-O(24)	2.279(6)	Dy(1)-O(25)	2.388(7)
Dy(1)-O(26)	2.491(10)				
O(23)-Dy(1)-O(23)	167.8(3)	O(23)-Dy(1)-O(24)	87.8(2)	O(23)-Dy(1)-O(24)	101.4(2)
O(23)-Dy(1)-O(25)	81.9(2)	O(23)-Dy(1)-O(25)	93.6(2)	O(23)-Dy(1)-O(26)	83.9(17)
O(24)-Dy(1)-O(24)	82.1(3)	O(24)-Dy(1)-O(25)	72.5(2)	O(24)-Dy(1)-O(25)	149.9(2)
O(24)-Dy(1)-O(26)	138.9(16)	O(25)-Dy(1)-O(25)	136.1(3)	O(25)-Dy(1)-O(26)	68.0(17)
3a					
Ho(1)-O(23)	2.242(5)	Ho(1)-O(24)	2.270(5)	Ho(1)-O(25)	2.368(6)
Ho(1)-O(26)	2.477(9)				
O(23)-Ho(1)-O(23)	168.1(3)	O(23)-Ho(1)-O(24)	88.2(19)	O(23)-Ho(1)-O(24)	100.8(2)
O(23)-Ho(1)-O(25)	93.5(2)	O(23)-Ho(1)-O(25)	82.0(2)	O(23)-Ho(1)-O(26)	84.1(15)
O(24)-Ho(1)-O(24)	82.2(3)	O(24)-Ho(1)-O(25)	72.2(2)	O(24)-Ho(1)-O(25)	150.3(2)
O(24)-Ho(1)-O(26)	138.9(14)	O(25)-Ho(1)-O(25)	136.1(3)	O(25)-Ho(1)-O(26)	68.1(15)
4a					
Er(1)-O(23)	2.223(5)	Er(1)-O(24)	2.271(5)	Er(1)-O(25)	2.361(5)
Er(1)-O(26)	2.462(8)				
O(23)-Er(1)-O(23)	168.3(3)	O(23)-Er(1)-O(24)	100.7(18)	O(23)-Er(1)-O(24)	88.2(18)
O(23)-Er(1)-O(25)	82.2(19)	O(23)-Er(1)-O(25)	93.4(19)	O(23)-Er(1)-O(26)	84.1(13)
O(24)-Er(1)-O(24)	82.4(3)	O(24)-Er(1)-O(25)	72.2(19)	O(24)-Er(1)-O(25)	150.6(19)
O(24)-Er(1)-O(26)	138.8(13)	O(25)-Er(1)-O(25)	135.8(3)	O(25)-Er(1)-O(26)	67.9(14)
1b					
Nd(1)-O(45)	2.417(12)	Nd(1)-O(46)	2.417(11)	Nd(1)-O(47)	2.402(11)
Nd(1)-O(48)	2.455(12)	Nd(1)-O(49)	2.385(10)	Nd(1)-O(50)	2.411(12)
Nd(1)-O(51)	2.413(12)	Nd(1)-O(52)	2.422(11)		
O(45)-Nd(1)-O(48)	141.9(4)	O(45)-Nd(1)-O(52)	77.9(4)	O(46)-Nd(1)-O(45)	78.4(4)

O(46)-Nd(1)-O(48)	73.2(4)	O(46)-Nd(1)-O(52)	73.8(4)	O(47)-Nd(1)-O(45)	72.9(4)
O(47)-Nd(1)-O(46)	77.3(4)	O(47)-Nd(1)-O(48)	76.4(4)	O(47)-Nd(1)-O(50)	141.5(4)
O(47)-Nd(1)-O(51)	115.8(4)	O(47)-Nd(1)-O(52)	142.3(4)	O(49)-Nd(1)-O(45)	112.4(4)
O(49)-Nd(1)-O(46)	143.4(4)	O(49)-Nd(1)-O(47)	73.4(4)	O(49)-Nd(1)-O(48)	79.0(4)
O(49)-Nd(1)-O(50)	78.5(4)	O(49)-Nd(1)-O(51)	71.4(4)	O(49)-Nd(1)-O(52)	141.4(4)
O(50)-Nd(1)-O(45)	143.6(5)	O(50)-Nd(1)-O(46)	114.3(4)	O(50)-Nd(1)-O(48)	72.9(4)
O(50)-Nd(1)-O(51)	78.0(4)	O(50)-Nd(1)-O(52)	73.9(4)	O(51)-Nd(1)-O(45)	73.5(4)
O(51)-Nd(1)-O(46)	142.9(4)	O(51)-Nd(1)-O(48)	141.8(4)	O(51)-Nd(1)-O(52)	76.9(4)
O(52)-Nd(1)-O(48)	116.7(4)				
4b					
Er(1)-O(45)	2.247(8)	Er(1)-O(48)	2.242(9)	Er(1)-O(51)	2.242(9)
Er(1)-O(54)	2.250(9)	Er(1)-O(57)	2.248(9)	Er(1)-O(60)	2.223(9)
Er(1)-O(63)	2.360(9)				
O(45)-Er(1)-O(54)	126.3(3)	O(45)-Er(1)-O(57)	146.4(4)	O(45)-Er(1)-O(63)	71.0(3)
O(48)-Er(1)-O(45)	76.3(3)	O(48)-Er(1)-O(51)	124.5(3)	O(48)-Er(1)-O(54)	76.4(3)
O(48)-Er(1)-O(57)	134.8(3)	O(48)-Er(1)-O(63)	135.0(3)	O(51)-Er(1)-O(45)	81.0(3)
O(51)-Er(1)-O(54)	77.7(3)	O(51)-Er(1)-O(57)	87.0(3)	O(51)-Er(1)-O(63)	79.9(3)
O(54)-Er(1)-O(63)	148.4(3)	O(57)-Er(1)-O(54)	80.7(3)	O(57)-Er(1)-O(63)	76.1(3)
O(60)-Er(1)-O(45)	101.5(4)	O(60)-Er(1)-O(48)	77.4(3)	O(60)-Er(1)-O(51)	157.5(4)
O(60)-Er(1)-O(54)	116.3(4)	O(60)-Er(1)-O(57)	78.7(4)	O(60)-Er(1)-O(63)	79.9(4)

Table S2 Weak interactions in the stacking structure of complex **1a**.

Intermolecular hydrogen bonds in the stacking structure of complex **1a**

Donor-H···Acceptor	D-H (Å)	H-A (Å)	D-A (Å)
O3-H3A···O20	0.85	2.30	2.773(14)
O4-H4A···N1S	0.86	2.38	2.739(19)
O4-H4B···N1S	0.84	1.97	2.739(19)
C1S-H1SB···O19	0.96	2.43	3.300(2)
C1S-H1SC···O5	0.96	2.56	3.340(2)
C9-H9···O17	0.93	2.59	3.462(18)
C10-H10···O16	0.93	2.49	3.066(14)
C27-H27···O16	0.93	2.52	3.302(19)
C34-H34···O21	0.93	2.59	3.271(14)

Intramolecular hydrogen bonding in the stacking structure of complex **1a**

Donor-H···Acceptor	D-H (Å)	H-A (Å)	D-A (Å)
O3-H3A···O4	0.85	2.29	2.774(11)
O4-H3B···O1	0.83	2.57	3.166(12)
C18-H18···O3	0.93	2.49	3.395(15)
C30-H30···O1	0.93	2.59	2.995(16)

Intramolecular π···π interactions in the stacking structure of complex **1a**

Cg(I)···Cg(J)	Cg(I)-Cg(J) (Å)	Cg(I) and Cg(J)
Cg(2)···Cg(2)	3.78(8)	Cg(2) = C7-C12

Intermolecular C-H···π interactions in the stacking structure of complex **1a**

C-H···Cg(I)	H···Cg (Å)	C-H···Cg (°)	C···Cg (Å)	Cg(I)
C3S-H3SA···Cg(3)	2.98	131	3.69(3)	Cg(3) = C13-C18

Intramolecular C-H···π interactions in the stacking structure of complex **1a**

C-H···Cg(I)	H···Cg (Å)	C-H···Cg (°)	C···Cg (Å)	Cg(I)
C24-H24···Cg(3)	2.78	133	3.48(12)	Cg(3) = C13-C18

Other weak interactions in the stacking structure of complex **1a**

Y-X···Cg(I)	X···Cg (Å)	Y-X···Cg (°)	Y···Cg (Å)	Cg(I)
C4S-N2S···Cg(1)	3.75(2)	84.60(14)	3.81(19)	Cg(1) = C1-C6

Table S3 Weak interactions in the stacking structure of complex **2a**.

Intermolecular hydrogen bonds in the stacking structure of complex **2a**

Donor-H···Acceptor	D-H (Å)	H-A (Å)	D-A (Å)
O25-H25C···O28	0.85	2.17	2.693(17)
O25-H25D···O14	0.85	1.92	2.752(11)
O27-H27C···O26	0.82	2.01	2.790(3)
O28-H28···O25	0.82	2.43	2.693(17)
C38-H38C···O22	0.96	2.56	3.240(8)

Intramolecular hydrogen bonding in the stacking structure of complex **2a**

Donor-H···Acceptor	D-H (Å)	H-A (Å)	D-A (Å)
O25-H25C···O24	0.85	2.38	2.760(10)
C36-H36···O25	0.93	2.53	3.444(13)

Intramolecular π···π interactions in the stacking structure of complex **2a**

Cg(I)···Cg(J)	Cg(I)-Cg(J) (Å)	Cg(I) and Cg(J)
Cg(5)···Cg(5)	3.78(6)	Cg(5) = C25-C30

Intermolecular C-H···π interactions in the stacking structure of complex **2a**

C-H···Cg(I)	H···Cg (Å)	C-H···Cg (°)	C···Cg (Å)	Cg(I)
C38-H38C···Cg(3)	2.90	138	3.67(7)	Cg(3) = C13-C18
C40-H40B···Cg(1)	2.93	132	3.65(2)	Cg(1) = C1-C6

Intramolecular C-H···π interactions in the stacking structure of complex **2a**

C-H···Cg(I)	H···Cg (Å)	C-H···Cg (°)	C···Cg (Å)	Cg(I)
C18-H18···Cg(6)	2.74	135	3.46(11)	Cg(6) = C31-C36
C30-H30···Cg(3)	2.98	115	3.47(12)	Cg(3) = C13-C18

Other weak interactions in the stacking structure of complex **2a**

Y-X···Cg(I)	X···Cg (Å)	Y-X···Cg (°)	Y···Cg (Å)	Cg(I)
Mo5-O19···Cg(4)	3.98(8)	106.1(3)	4.71(5)	Cg(4) = C19-C24

Table S4 Weak interactions in the stacking structure of complex **3a**.

Intermolecular hydrogen bonds in the stacking structure of complex **3a**

Donor-H···Acceptor	D-H (Å)	H-A (Å)	D-A (Å)
O25-H25C···O28	0.85	2.16	2.690(15)
O25-H25D···O14	0.85	1.94	2.768(9)
O27-H27C···O26	0.82	2.02	2.800(3)
O28-H28···O25	0.82	2.42	2.690(15)
C3-H3···O10	0.93	2.60	3.500(14)

Intramolecular hydrogen bonding in the stacking structure of complex **3a**

Donor-H···Acceptor	D-H (Å)	H-A (Å)	D-A (Å)
O25-H25C···O24	0.85	2.35	2.736(8)
C36-H36···O25	0.93	2.53	3.441(11)

Intramolecular π···π interactions in the stacking structure of complex **3a**

Cg(I)···Cg(J)	Cg(I)-Cg(J) (Å)	Cg(I) and Cg(J)

Cg(5)···Cg(5)	3.77(6)	Cg(5) = C25-C30

Intermolecular C-H···π interactions in the stacking structure of complex **3a**

C-H···Cg(I)	H···Cg (Å)	C-H···Cg (°)	C···Cg (Å)	Cg(I)
C38-H38C···Cg(3)	2.79	152	3.66(7)	Cg(3) = C13-C18

Intramolecular C-H···π interactions in the stacking structure of complex **3a**

C-H···Cg(I)	H···Cg (Å)	C-H···Cg (°)	C···Cg (Å)	Cg(I)
C18-H18···Cg(6)	2.73	136	3.46(11)	Cg(6) = C31-C36
C30-H30···Cg(3)	2.97	116	3.47(10)	Cg(3) = C13-C18

Other weak interactions in the stacking structure of complex **3a**

Y-X···Cg(I)	X···Cg (Å)	Y-X···Cg (°)	Y···Cg (Å)	Cg(I)
Mo5-O19···Cg(4)	3.98(8)	106.1(3)	4.71(4)	Cg(4) = C19-C24

Table S5 Weak interactions in the stacking structure of complex **4a**.

Intermolecular hydrogen bonds in the stacking structure of complex **4a**

Donor-H···Acceptor	D-H (Å)	H-A (Å)	D-A (Å)
O25-H25C···O28	0.85	2.16	2.682(15)
O25-H25D···O14	0.85	1.94	2.770(9)
O27-H27C···O26	0.82	2.02	2.800(3)
O28-H28···O25	0.82	2.42	2.682(15)
C3-H3···O10	0.93	2.60	3.495(13)

Intramolecular hydrogen bonding in the stacking structure of complex **4a**

Donor-H···Acceptor	D-H (Å)	H-A (Å)	D-A (Å)
O25-H25C···O24	0.85	2.35	2.730(7)
C36-H36···O25	0.93	2.53	3.435(10)

Intramolecular π···π interactions in the stacking structure of complex **4a**

Cg(I)···Cg(J)	Cg(I)-Cg(J) (Å)	Cg(I) and Cg(J)
Cg(5)···Cg(5)	3.77(5)	Cg(5) = C25-C30

Intermolecular C-H···π interactions in the stacking structure of complex **4a**

C-H···Cg(I)	H···Cg (Å)	C-H···Cg (°)	C···Cg (Å)	Cg(I)

C38-H38C···Cg(3)	2.94	141	3.73(11)	Cg(3) = C13-C18
C40-H40B···Cg(1)	3.00	127	3.65(2)	Cg(1) = C1-C6
Intramolecular C-H···π interactions in the stacking structure of complex **4a**				
C-H···Cg(I)	H···Cg (Å)	C-H···Cg (°)	C···Cg (Å)	Cg(I)
C18-H18···Cg(6)	2.72	137	3.46(9)	Cg(6) = C31-C36
C30-H30···Cg(3)	3.00	113	3.48(9)	Cg(3) = C13-C18
Other weak interactions in the stacking structure of complex **4a**				
Y-X···Cg(I)	X···Cg (Å)	Y-X···Cg (°)	Y···Cg (Å)	Cg(I)
Mo5-O19···Cg(4)	3.99(8)	105.8(3)	4.71(4)	Cg(4) = C19-C24

Table S6 Weak interactions in the stacking structure of complex **1b**.

Intermolecular hydrogen bonds in the stacking structure of complex **1b**			
Donor-H···Acceptor	D-H (Å)	H-A (Å)	D-A (Å)
C(2)-H(2A)···O(15)	0.97	2.42	3.29(2)
C(3)-H(3B)···O(14)	0.97	2.53	3.38(2)
C(11)-H(11A)···O(13)	0.97	2.42	3.25(2)
C(17)-H(17A)···O(5)	0.97	2.51	3.42(3)
C(18)-H(18B)···O(21)	0.96	2.40	3.32(2)
C(22)-H(22A)···O(37)	0.97	2.50	3.40(2)
C(23)-H(23B)···O(30)	0.97	2.53	3.29(2)
C(23)-H(23B)···O(44)	0.97	2.50	3.27(2)
C(32)-H(32A)···O(44)	0.97	2.25	3.21(3)
C(36)-H(36B)···O(34)	0.96	2.59	3.47(3)
C(42)-H(42A)···O(22)	0.96	2.52	3.44(3)
Intramolecular hydrogen bonding in the stacking structure of complex **1b**			
Donor-H···Acceptor	D-H (Å)	H-A (Å)	D-A (Å)
C(3)-H(3A)···O(54)	0.97	2.57	2.96(3)
C(13)-H(13A)···O(58)	0.97	2.60	3.00(2)
C(17)-H(17B)···O(48)	0.97	2.56	2.96(2)
C(25)-H(25A)···O(49)	0.97	2.35	2.86(3)
C(33)-H(33A)···O(66)	0.97	2.50	2.95(3)
C(37)-H(37A)···O(52)	0.97	2.26	2.73(3)

Table S7 Weak interactions in the stacking structure of complex **4b**

Intermolecular hydrogen bonds in the stacking structure of complex **4b**

Donor-H···Acceptor	D-H (Å)	H-A (Å)	D-A (Å)
O(63)-H(63C)···N(1)	0.85	1.97	2.81(2)
O(63)-H(63D)···O(19)	0.85	2.07	2.897(15)
C(1)-H(1A)···O(38)	0.97	2.55	3.325(17)
C(1)-H(1B)···O(14)	0.97	2.43	3.365(18)
C(2)-H(2B)···O(35)	0.97	2.54	3.370(17)
C(12)-H(12B)···O(31)	0.97	2.58	3.47(2)
C(14)-H(14B)···O(10)	0.96	2.51	3.45(2)
C(19)-H(19B)···O(31)	0.97	2.50	3.216(19)
C(25)-H(25A)···O(34)	0.97	2.55	3.50(2)
C(26)-H(26B)···O(38)	0.96	2.47	3.38(3)
C(26)-H(26C)···O(16)	0.96	2.44	3.19(3)
C(29)-H(29B)···O(16)	0.97	2.45	3.41(3)
C(32)-H(32A)···O(12)	0.96	2.54	3.46(2)

Intramolecular hydrogen bonding in the stacking structure of complex **4b**

Donor-H···Acceptor	D-H (Å)	H-A (Å)	D-A (Å)
C(1)-H(1B)···O(50)	0.97	2.59	3.065(17)
C(7)-H(7B)···O(56)	0.97	2.52	3.229(18)
C(17)-H(17A)···O(58)	0.97	2.56	3.46(2)
C(23)-H(23A)···O(59)	0.97	2.51	2.86(2)
C(25)-H(25B)···O(57)	0.97	2.60	2.94(2)
C(27)-H(27A)···O(60)	0.97	2.58	3.01(3)

Table S8 Comparison of the photocatalytic activities of the selected lanthanide polyacid complexes.

Photocatalyst	Light source	Band gap (eV)	Degradation rate	Stability (cycle)	Ref.
$(enH_2)_2[Cu(en)_2]\{[Cu(en)_2]_{1.5}[Cu(en)(2,2'\text{-bipy})]Ce[(\alpha\text{-}PW_{11}O_{39})_2]\}\bullet 2H_2O$	500 W Hg lamp UV	-	210 min RhB (26%)	1	34
$(enH_2)_2[Cu(en)_2(H_2O)]\{[Cu(en)_2]_{1.5}[Cu(en)(2,2'\text{-bipy})(H_2O)]Pr[(\alpha\text{-}PW_{11}O_{39})_2]\}\bullet 6.5H_2O$	500 W Hg lamp UV	-	210 min RhB (34%)	1	34
$[Cu(en)_2(H_2O)_2][Cu(en)(2,2'\text{-bipy})(H_2O]\{[Cu(en)_2]_2(H_2O)[Cu(en)(2,2'\text{-bipy})]Gd[(\alpha\text{-}HPW_{11}O_{39})_2]\}\bullet 6H_2O$	500 W Hg lamp UV	-	210 min RhB (29%)	1	34
$[Cu(en)_2(H_2O)_2][Cu(en)(2,2'\text{-bipy})(H_2O]\{[Cu(en)_2]_2[Cu(en)(2,2'\text{-bipy})]Tb[(\alpha\text{-}HPW_{11}O_{39})_2]\}\bullet 7.5H_2O$	500 W Hg lamp UV	-	210 min RhB (35%)	1	34
$[Cu(en)_2(H_2O)][Cu(en)(2,2'\text{-bipy})(H_2O]\{[Cu(en)_2]_2(H_2O)[Cu(en)(2,2'\text{-bipy})]Er[(\alpha\text{-}HPW_{11}O_{39})_2]\}\bullet 7.5H_2O$	500 W Hg lamp UV	-	210 min RhB (46%)	1	34
$\{[Sm(H_2O)_4(pdc)]_3\}\{[Sm(H_2O)_3(pdc)]\}[SiMo_{12}O_{40}]\cdot 3H_2O$	175 W UV	-	120 min RhB (70.1%)	4	35
$\{[La(H_2O)_4(pdc)]_4\}[PMo_{12}O_{40}]F$	175 W UV	-	120 min RhB (75.3%)	4	35
$[La(HL)(L)(H_2O)_6\{La(H_2L)_{0.5}(\alpha\text{-}PW_{11}O_{39}H)La(H_2O)_4\}]_2\cdot 8H_2O$	500 W Hg lamp UV	-	240 min RhB (59.8%)	1	21

$[Ce(HL)(L)(H_2O)_6\{Ce(H_2L)_{0.5}(\alpha\text{-}PW_{11}O_{39}H)Ce(H_2O)_4\}]_2\cdot 12H_2O$	500 W Hg lamp UV	-	240 min RhB (56.0%)	1	21
$[Pr(HL)(L)(H_2O)_6\{Pr(H_2L)_{0.5}(\alpha\text{-}PW_{11}O_{39}H)Pr(H_2O)_4\}]_2\cdot 8H_2O$	500 W Hg lamp UV	-	240 min RhB (45.2%)	1	21
$Na[Cu(en)_2(H_2O)]_4[Cu(en)_2]_2[Cu(H_2O)_4]_{0.5}\{Cu(en)_2[H_2Ce(\alpha\text{-}AsW_{11}O_{39})_2]_2\}\cdot 10H_2O$	500 W Hg lamp UV	-	420 min RhB (30.2%)	1	36
$Na_3[Cu(en)_2(H2O)][Cu(en)_2]_{1.5}[H_3Pr(\alpha\text{-}AsW_{11}O_{39})_2]\cdot 5H_2O$	500 W Hg lamp UV	-	420 min RhB (27.3%)	1	36
$[Cu(dap)(H2O)_2]_{0.5}[Cu(dap)_2(H_2O)]_2[Cu(dap)_2]_3[Pr(\alpha\text{-}AsW_{11}O_{39})_2]\cdot 3H_2O$	500 W Hg lamp UV	-	420 min RhB (30.0%)	1	36
$[Cu(dap)_2]_{5.5}[Tb(\alpha\text{-}AsW_{11}O_{39})_2]\cdot 6H_2O$	500 W Hg lamp UV	-	420 min RhB (32.5%)	1	36
$[Gd(H_2O)_7][Gd(H_2O)_5][Co_2Mo_{10}H_4O_{38}]\cdot 5H_2O$	500 W Xe lamp Vis	-	540 min MO (69.0%)	4	37
$[Tb(H_2O)_7][Tb(H_2O)_5][Co_2Mo_{10}H_4O_{38}]\cdot 5H_2O$	500 W Xe lamp Vis	-	540 min MO (62.0%)	4	37
$[Gd(H_2O)_7][Gd(H_2O)_5][Co_2Mo_{10}H_4O_{38}]\cdot 5H_2O$	500 W Xe lamp Vis	-	540 min RhB (77.1%)	4	37
$[Tb(H_2O)_7][Tb(H_2O)_5][Co_2Mo_{10}H_4O_{38}]\cdot 5H_2O$	500 W Xe lamp Vis	-	540 min RhB	4	37

			(73.8%)		
$[Nd(OPPh_3)_4(H_2O)_3](PMo_{12}O_{40})\cdot 4CH_3CN$	400 W Hg lamp UV	2.49 eV	90 min MB (99.30%)	5	This work
$[Ln(OPPh_3)_4(H_2O)_3](PMo_{12}O_{40})\cdot 4CH_3CH_2OH$ (Ln = Dy, Ho, Er)	400 W Hg lamp UV	2.41-2.63 eV	90 min MB (94.93%-99.55%)	5	This work
$[Ln(OPPh_3)_4(H_2O)_3](PW_{12}O_{40})\cdot 4CH_3CN$ (Ln=La,Nd)	300 W Xe lamp UV	around 3.1 eV	120minMB（99.00%）	5	Other research in our group